Journal of Photochemistry and Photobiology A: Chemistry 200 (2008) 318–324

Contents lists available at ScienceDirect

Journal of Photochemistry and Photobiology A: Chemistry

journal homepage: www.elsevier.com/locate/jphotochem

Synthesis and photophysical properties of novel organic–inorganic hybrid materials covalently linked to a europium complex

Xianmin Guo[a,b], Huadong Guo[a,b], Lianshe Fu[c], Hongjie Zhang[a,*], L.D. Carlos[c], Ruiping Deng[a], Jiangbo Yu[a]

[a] State Key Laboratory of Application of Rare Earth Resources, Changchun Institute of Applied Chemistry, Chinese Academy of Sciences, 5625 Remin Street, Changchun 130022, PR China
[b] Graduate School of the Chinese Academy of Sciences, Changchun 130022, PR China
[c] Department of Physics, CICECO, University of Aveiro, 3810-193 Aveiro, Portugal

ARTICLE INFO

Article history:
Received 29 March 2008
Received in revised form 29 July 2008
Accepted 16 August 2008
Available online 3 September 2008

Keywords:
Organic–inorganic hybrid composite
Photophyscial property
β-Diketone
Europium complex

ABSTRACT

A novel sol–gel derived hybrid material (classed as Eu-DBM-Si) covalently grafted with Eu(DBM-OH)$_3$·2H$_2$O (where DBM-OH = *o*-hydroxydibenzoylmethane) was prepared through the primary β-diketone ligand DBM-OH. All the synthesized ligands were characterized by ^{1}H NMR, elemental analyses and Fourier transform infrared spectra (FTIR). The resultant Eu-DBM-Si material exhibited good transparent and homogenous property. Compared to the Eu-DBM hybrid prepared by physically doped silicon dioxide with Eu(DBM-OH)$_3$·2H$_2$O, the Eu-DBM-Si hybrid presented more efficient ligand-to-Eu^{3+} energy transfer and a significant improvement in the measured emission quantum yield. Furthermore, the photophysical properties of these hybrid materials, such as the photoluminescence (PL) spectra, PL intensities, symmetry properties, lifetime decays, and Judd-Ofelt parameters were also investigated in detail.

1. Introduction

Luminescent lanthanide complexes are interesting materials not only due to their academic importance but essentially to a variety of potential technological applications, such as in fluoroimmunoassays, spectroscopic structural probes in biologically important systems, lasers, optical amplification and organic light-emitting diodes [1–5]. The intrinsic photophysical properties of the trivalent lanthanide ions, such as line-like emission spectra, high-luminescence quantum efficiency, and large Stokes shifts [6–9], enable them as ideal candidates as emitting centers for those applications. However, lanthanide complexes have been excluded so far from practical applications essentially owing to their poor thermal stabilities under heating or moisture and low mechanical strength [10]. In order to overcome these drawbacks, lanthanide complexes have been incorporated into inert host matrices, for example, silica-based materials [11–22], polymers [23–27] or liquid crystal [28–31], forming the so-called "organic–inorganic hybrid materials". The sol–gel method is an attractive technique for preparing these organic–inorganic hybrid materials combining the inorganic and organic precursor components at the nanometer scale [32,33]. The sol–gel derived organic–inorganic hybrid materials can thus exhibit excellent mechanical properties and good thermal and photo stabilities [34–39].

Up to now, two main approaches have been proposed to incorporate lanthanide complexes into sol–gel derived materials: (i) direct dissolution of the complex into the hybrid host or its in situ synthesis during the sol–gel process through weak physical interactions (van der Waals force, hydrogen bonding, or weak static effect) [18,19,40]; (ii) covalent grafting of the complex into the sol–gel matrix through hydrolysis and condensation of double functional trialkoxysilyl units [14,15,20–22]. In the first strategy it is difficult to obtain a uniform distribution of the lanthanide complex due to their low solubility and/or poor stability in the sol–gel precursor solutions, while transparent, homogeneously dispersed and monolithic composites can be obtained and the self-quenching resulting from concentration effects can be avoided through the second approach. Therefore, a large degree of attention was presently devoted to attaching the lanthanide complex with sol–gel derived host structures by covalent bonds. Ternary lanthanide (III) complexes with β-diketones have been usually linked to sol–gel derived matrices hydrolyzing and condensing the double functional synergic ligand, such as 1,10-phenanthroline [14,15,41,42] and 4, 4′-bipyridine [20,22], and then binary β-diketone complexes are introduced by ligand exchange reactions. Obviously, it can not be assured that all the binary lanthanide complexes are grafted into the functionalized

* Corresponding author. Tel.: +86 431 85262127; fax: +86 431 85698041.
E-mail address: hongjie@ciac.jl.cn (H. Zhang).

1010-6030/$ – see front matter © 2008 Elsevier B.V. All rights reserved.
doi:10.1016/j.jphotochem.2008.08.016

host matrix through covalent bonds (perhaps part of the binary lanthanide complexes is introduced by simple physical methods, leading to their relatively inhomogeneous distribution). Thus, the direct covalent grafting of the primary ligand β-diketones into the inorganic host matrix may overcome the disadvantages of the above approach. To the best of our knowledge, the method of covalently bonded sol–gel matrices with modified primary β-diketones ligands, such as dibenzoylmethane (DBM), has rarely been reported in the open literature so far.

In the present paper, we report the synthesis of a europium complex functionalized sol–gel hybrid in which DBM-OH was covalently bonded to the matrix framework through hydrolysis and condensation of modified DBM-OH *o*-(O-3-(triethoxysilyl)propyl)aminocarbonyl-dibenzoylmethane (DBM-Si) and tetrethoxysilane (TEOS) in the presence of lanthanide ions (in situ approach). The resultant Eu-DBM-Si organic–inorganic hybrid materials display excellent homogeneousness and transparence and their luminescence properties were improved in comparison with the physically doped Eu-DBM hybrid.

2. Experimental

2.1. Materials

3-(Triethoxysilyl)-propyl isocyanate (ICPTES, Aldrich), *o*-hydroxyacetophenone, benzoyl chloride (A.R. grade, Shanghai, China), tetraethylorthosilicate (TEOS, Beijing, China), potassium hydroxide (KOH), hydrochloric acid (HCl) and *N*,*N*-dimethylformamide (DMF) were commercially available and used without further purification. Petroleum ether and triethylamine were desiccated with anhydrous calcium chloride and sodium hydroxide for several days prior to use, respectively. Pyridine was distilled after desiccation with KOH for 24 h. Tetrahydrofuran (THF) was stirred with sodium-benzophenone and distilled. Ethanol (EtOH) was distilled after desiccation with calcium oxide. Europium (III) chloride ($EuCl_3{\cdot}6H_2O$) was obtained by reaction of europium oxide (Eu_2O_3, 99.99%, Shanghai, China) with HCl and dissolved in EtOH. Distilled water was used throughout the experiments.

2.2. Synthesis of DBM-Si

The schematic diagram of synthetic procedure for the original material DBM-OH and other products is shown in Scheme 1.

DBM-OH was synthesized according to the method described in literature [43], which was characterized by ^{1}H-NMR and FTIR spectra. ^{1}H NMR ($CDCl_3$, 400 MHz) δ (ppm): 15.65 (1H, s, OH of enol), 12.09 (1H, s, OH of hydroxybenzene), 7.91–8.02 (2H, dd, ArH), 7.73–7.87 (1H, dd, ArH), 7.39–7.64 (4H, m, ArH), 6.99–7.08 (1H, d, ArH), 6.91–6.99 (1H, m, ArH), 6.87 (1H, s, CH of enol). FTIR (KBr, cm^{-1}): 1607, 1573 and 1489. Elemental analysis: calculated: C, 75.00%; H, 5.00%. Found: C, 74.89%; H, 5.09%. DBM-Si was prepared as follows: triethylamine (10 mmol) and ICPTES (15 mmol) were added under nitrogen to a solution of DBM-OH (10 mmol) in anhydrous THF (10 mL). The mixture was heated under reflux for 24 h. Then, the mixture was added dropwise into petroleum ether under stirring by glass rod. The resulting white precipitate was filtered off, washed with petroleum ether for 4 times and dried at 50 °C in vacuum for 10 h. DBM-Si was also characterized by ^{1}H-NMR spec-

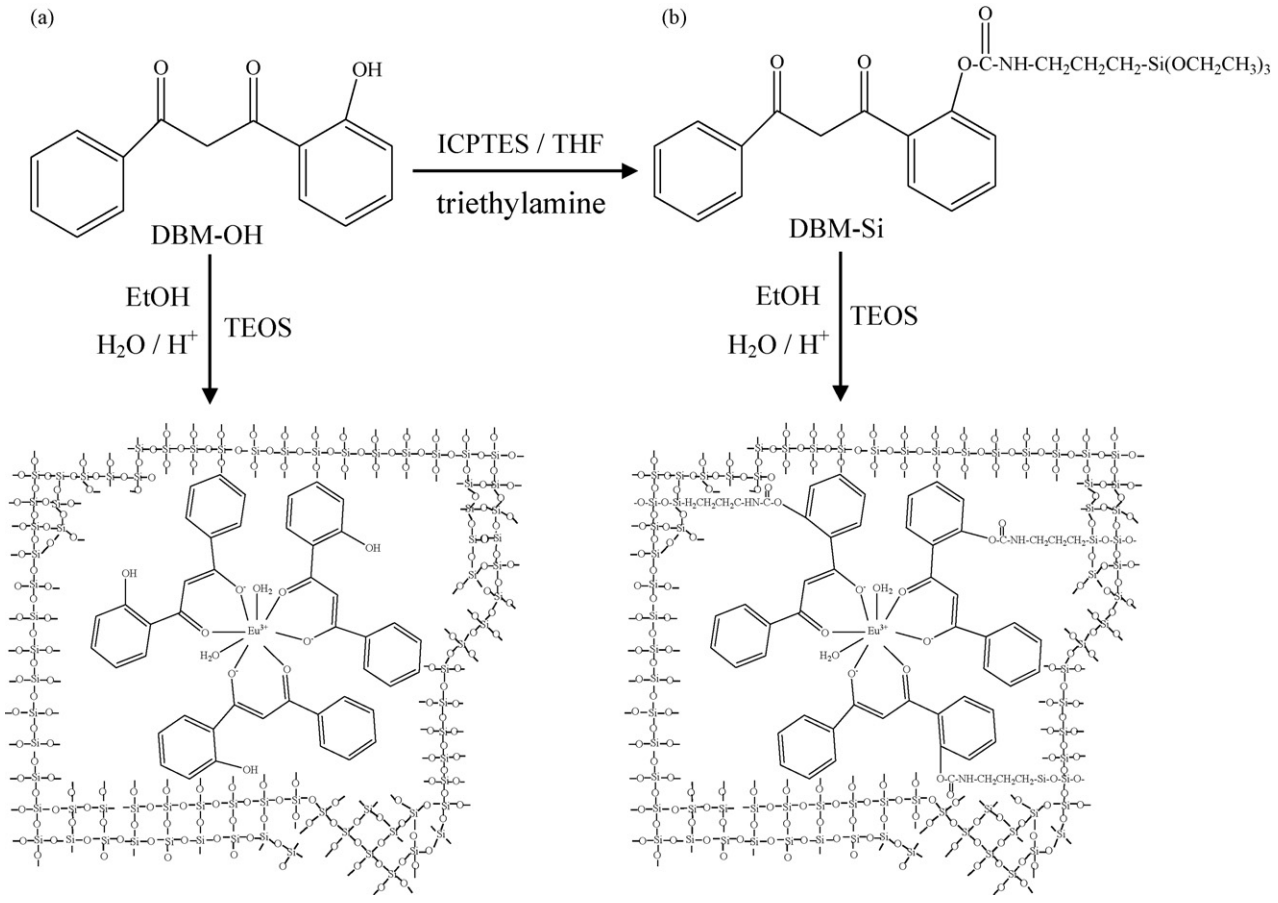

Scheme 1. Schematic diagram of synthetic procedure and the possible structures for the hybrid materials Eu-DBM (a) and Eu-DBM-Si (b).

trum. ^{1}H NMR(DMSO, 400 MHz) δ (ppm): 16.12 (1H, s, OH of enol), 8.40 (1H, t, NH), 8.13–8.17 (1H, dd, ArH), 7.90–7.93 (3H, m, ArH), 7.80–7.82 (1H, d, ArH), 7.57–7.65 (5H, m, ArH and CH of enol), 3.77 (6H, q, OCH_2), 3.08 (2H, q, NCH_2), 1.46 (2H, quint, CH_2), 1.20 (9H, t, CH_3),0.53 (2H, t, $SiCH_2$). Elemental analysis: calculated: C, 61.60%; H, 6.78%; N, 2.87%. Found: C, 61.52%; H, 6.75%; N, 2.92%.

2.3. Synthesis of the matrix, hybrid materials covalently bonded with europium complex ligand (Eu-DBM-Si (x)) and hybrid materials physically doped with Eu(DBM-OH)$_3$·2H$_2$O complex (Eu-DBM)

A series of Eu-DBM-Si (x) hybrid materials (x = 0.25%, 0.5%, 0.75%, 1.0%, where x is the molar ratio of Eu^{3+}/(TEOS + DBM-Si)) in situ synthesized *via* sol–gel process were prepared as follows: the molar ratio of TEOS:EtOH:H_2O (0.01 M HCl) in original solution was 1:4:4. Then an appropriate amount of DBM-Si was introduced into the solution. Upon resulting a clear sol, $EuCl_3$ ethanol solution was added with a molar ratio of Eu^{3+}:DBM-Si = 1:3. The mixed solution was agitated magnetically for several hours at room temperature to obtain a single phase, and then transferred to a plastic container with some holes on the cover. The sol converted to colorless transparent monolithic gel after several days of gelation at 40 °C. When Eu ion was not added in the precursor solution, we got the matrix material, designated as DBM-Si. The synthesis procedure for Eu-DBM was similar to that of Eu-DBM-Si except DBM-OH instead of DBM-Si. The possible structures for the hybrid materials Eu-DBM (a) and Eu-DBM-Si (b) were also shown in Scheme 1.

2.4. Synthesis of Gd(DBM-OH)$_3$·2H$_2$O and Gd(DBM-Si)$_3$·2H$_2$O complexes

At room temperature, 3 mmol of DBM-OH was dissolved in a certain amount of anhydrous ethanol. Then 1 mmol of $GdCl_3$ ethanol solution was added under stirring for 5 h. The yellow powder was filtered and washed with ethanol. The resulting Gd(DBM-OH)$_3$·2H$_2$O was dried at 60 °C under vacuum overnight. The synthesis method of Gd(DBM-Si)$_3$·2H$_2$O was similar to the above procedure. The obtained power was dissolved in anhydrous DMF for characterization.

2.5. Characterization

Diffuse reflection UV–visible (DR UV–vis) spectrum was acquired from Hitachi F-4100 with tungsten and deuterium lamps. Fourier transform infrared spectra (FTIR) were measured on a Bruker Vertex 70 Spectrophotometer within the wavenumber range 4000–400 cm^{-1} at a resolution of 4 cm^{-1} using KBr pressed pellet technique. TG analysis was performed on an SDT 2960 analyzer (Shimadzu, Japan) from 45 to 900 °C at a heating speed of 10 °C/min under air atmosphere. The fluorescence excitation and emission spectra were recorded on a JY FL-3 spectrophotometer equipped with a 450 W Xenon lamp as an excitation source. Luminescence lifetime was measured with a Lecroy Wave Runner 6100 Digital Oscilloscope (1 GHz) using different wave-number lasers (Continuum Sunlite OPO with pulse width = 4 ns) as an excitation source. The low temperature phosphorescence spectrum of Gd^{3+} complex was measured on a Hitachi F-4500 spectrophotometer at liquid nitrogen temperature (77 K). The PL quantum yield (Φ) was measured with an integrating sphere (Power Technology Inc.) using a 325 nm HeCd laser (Kimmom, Japan) as an excitation source. Elemental analyses of carbon, hydrogen, and nitrogen were carried out on a VarioEL analyzer.

3. Results and discussion

3.1. In situ synthesis of hybrid materials either covalently linked or physically doped with europium β-diketonate complex

During the conversion process of sol to xerogel, the binary europium complex with DBM was in situ synthesized accompanied with the evaporation of residual HCl and ethanol. Finally, within the investigated concentration of europium complex, monolithic gels with good transparency were obtained. Under UV irradiation, the resultant hybrid materials Eu-DBM-Si and Eu-DBM exhibit the characteristic emission of Eu^{3+} ion. The photographs for Eu-DBM-Si (0.5%) before and under UV irradiation are shown in Fig. 1.

3.2. FTIR spectra

The FTIR spectra of ICPTES (a), DBM-Si (b), Eu-DBM-Si (0.5%) (c) and Eu-DBM (d) are shown in Fig. 2. In Fig. 2a and b, the disappearance of peak at 2273 cm^{-1} (ν, –N=C=O) and emergence of bands at 1647 cm^{-1} (ν, O=C–NH), 1397, 1571 cm^{-1} (δ, C–N), 1535, 3266 cm^{-1}(ν, N–H) and 1632 cm^{-1} (ν, C=O) indicate the success of the grafting reaction [21,41]. Moreover, the spectrum of DBM-Si is dominated by 1191 cm^{-1} (ν, C–Si) and 1070 cm^{-1} (ν, Si–OEt) absorption bands, characteristic of trialkoxysilyl functions. In Fig. 2c and d, the formation of Si–O–Si framework is evidenced by the bands located at 1075, 1080 cm^{-1} (ν_{as}, Si–O–Si), 793, 795 cm^{-1} (ν_s, Si–O–Si) and 449, 455 cm^{-1} (δ, Si–O–Si) (ν = stretching, δ = in-plane bending, s = symmetric and as = asymmetric vibrations). The existence of β-diketone can be confirmed by 1566, 1626 cm^{-1} (ν, C=O, the latter only seen in Fig. 2d), 1449, 1454 cm^{-1} (ν, C=O or δ, C–H) and 1483, 1486 cm^{-1} ($\varphi\nu$, C=C) (φ = phenyl vibrations). The peaks at 1638, 1540 and 1397 cm^{-1}, originating from C=O, N–H and C–N of the –CONH– group of DBM-Si, can still be observed in Fig. 2c, indicating the fact that DBM-Si remains intact after the hydrolysis/condensation reaction.

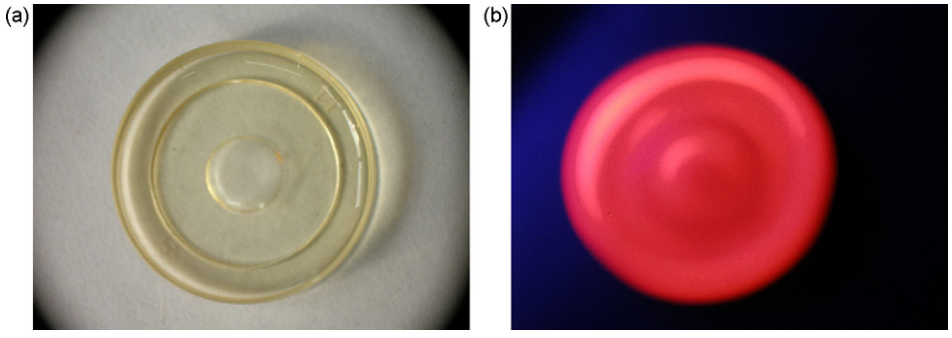

Fig. 1. Photographs of Eu-DBM-Si (0.5%) without UV irradiation (a) and under UV irradiation (b).

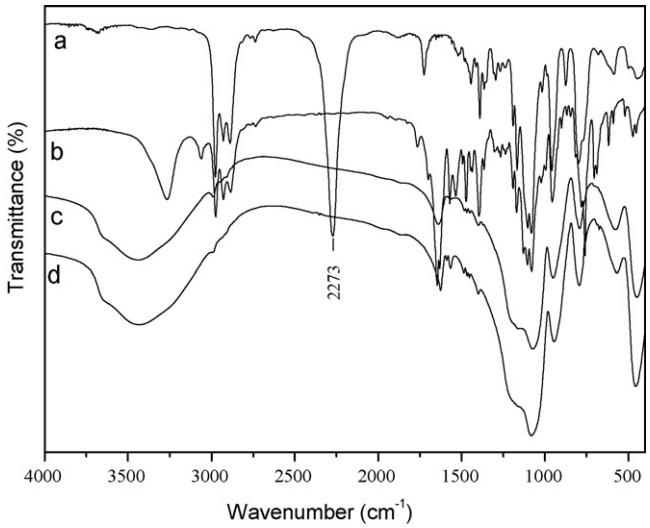

Fig. 2. FTIR spectra of ICPTES (a), DBM-Si (b), Eu-DBM-Si (0.5%) (c) and Eu-DBM (0.5%) (d).

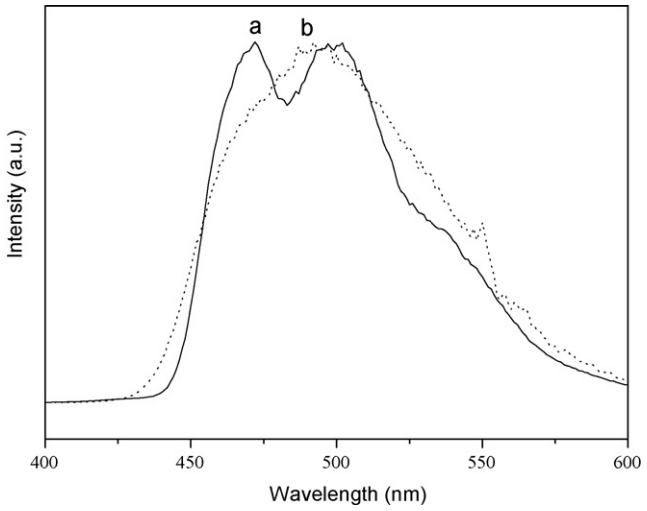

Fig. 4. PL spectra of $Gd(DBM\text{-}OH)_3{\cdot}2H_2O$ (a, λ_{ex} = 305 nm, solid line) and $Gd(DBM\text{-}Si)_3{\cdot}2H_2O$ (b, λ_{ex} = 310 nm, dotted line) at 77 K in 1.0×10^{-4} M DMF solution.

3.3. Antenna effects

The excitation spectrum of the resulting Eu-DBM-Si hybrid (detected at 612 nm) and DR UV–vis absorption spectrum of DBM-Si are shown in Fig. 3. It can be clearly seen that there is a large overlap between the excitation band of Eu-DBM-Si (Fig. 3a) and the absorption band of DBM-Si (Fig. 3b), which suggests that the central Eu^{3+} ion in Eu-DBM-Si can be efficiently sensitized by the ligands, an "antenna effect" [44–48].

In order to further investigate this efficient ligand-to-metal ion energy transfer, the triplet state energy levels of the DBM-OH and DBM-Si ligands were both measured (the energy transfer is based on the energy difference between the triplet state of the ligand and the resonance energy level of the central lanthanide ion). Sato et al. reported that too large or too small energy differences decrease the efficiency of the ligand-to-metal energy transfer [47,49–51]. The suitable energy difference for an efficient ligand-to-Eu^{3+} intramolecular energy transfer lies in the range of 500–2500 cm^{-1} [49]. The triplet state energy levels of DBM-OH and DBM-Si ligands were determined from the phosphorescence spectra of the respective Gd^{3+} complexes owing to their enhanced phosphorescence–fluorescence ratio ($\Phi_p/\Phi_f > 100$) compared to those of other lanthanide chelate complexes at 77 K under UV excitation [47]. The corresponding phosphorescence emission spectra are displayed in Fig. 4, which are excited at 305 and 310 nm, respectively. The triplet state energy levels are determined from the corresponding shortest-wavelength phosphorescence band (21,186 and 20,325 cm^{-1}, respectively), which is assumed to be the 0–0 transition of the ligand. In addition, the resonance $^5D_1$ energy level of Eu^{3+} is 19,020 cm^{-1} [41,50]. Therefore, the energy differences between the triplet state energy levels of DBM-OH and DBM-Si and the $^5D_1$ level are 2166 and 1305 cm^{-1}, respectively. According to the luminescence theory of lanthanide complexes, the ligands DBM-OH and DBM-Si can both efficiently sensitize the luminescence of the central Eu^{3+} ions. Whereas, it is also worth noting that the energy difference between the triplet state energy level of DBM-Si ligand and the $^5D_1$ level of Eu^{3+} ion is able to be comparable with that between the traditional ligand 4,4,4-trifluoro-1-(2-thienyl)butane-1,3-dione (TTA) and the $^5D_1$ level of Eu^{3+} ion [47]. As well known, TTA is an efficient sensitizer for the luminescence of central Eu^{3+} ion, which can efficiently transfer the energy to Eu^{3+} ion. Therefore, we might conclude that the intramolecular energy transfer between the DBM-Si ligand and the Eu^{3+} ion is more efficient than that between DBM-OH and Eu^{3+} ion, which indicates that the DBM-OH functionalization contributes to the improvement of its sensitive efficiency, relatively to Eu^{3+}. This is in satisfactory agreement with the results of the luminescence section.

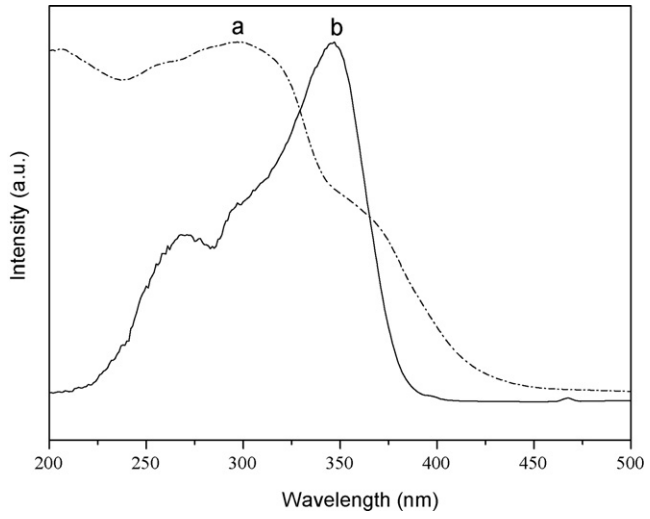

Fig. 3. DR UV–vis absorption spectrum of DBM-Si (a, dashed line) in the solid; excitation spectrum for Eu-DBM-Si (0.5%) (b, solid line) detected at 612 nm in the solid. All spectra are normalized to a constant intensity at the maximum.

3.4. Doping concentration selecting of europium complex

In order to select a suitable doping concentration of europium complex in silicon dioxide matrix, different concentrations of $EuCl_3$ and DBM-Si were incorporated into solid matrice in the range of 0.25–1.0% (molar ratio of Eu^{3+}: Si in sols, a similar concentration range to the literature [33]) to form Eu-DBM-Si, as described in Section 2. The corresponding room temperature emission spectra measured in same conditions are shown in Fig. 5. The intensity of the emission spectrum increases gradually as the Eu^{3+} concentration increases reaching a plateau for concentrations higher than 0.5%. Consequently, this was the doping concentration of the silicon dioxide hybrid doped with $Eu(DBM\text{-}OH)_3{\cdot}2H_2O$ complex (denoted as Eu-DBM).

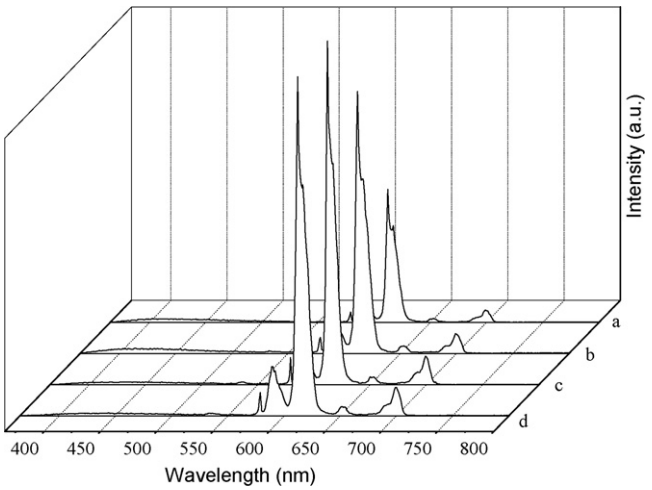

Fig. 5. PL spectra of Eu-DBM-Si (x) x = 0.25% (a), 0.5% (b), 0.75% (c) and 1.0% (d).

3.5. Photoluminescence (PL) spectra

The emission spectra for Eu-DBM, Eu-DBM-Si and DBM-Si are presented in Fig. 6, which were obtained by irradiation of the samples using maximum excitation wavelengths of 350, 350 and 330 nm, respectively. The spectra clearly exhibit the intra-4f^6 $^5D_0 \rightarrow {}^7F_J$ (J = 0, 1, 2, 3, 4) Eu^{3+} transitions, with the $^5D_0 \rightarrow {}^7F_2$ emission as the dominant band. Meanwhile, two weak bands at 535 and 553 nm were also observed which are tentatively assigned to the $^5D_1 \rightarrow {}^7F_1$ and $^5D_1 \rightarrow {}^7F_2$ transitions, respectively. Furthermore, in the corresponding emission spectrum of Eu-DBM, besides the Eu^{3+} $^5D_0 \rightarrow {}^7F_{0-4}$ and $^5D_1 \rightarrow {}^7F_{1,2}$ transitions, a broad emission band in the blue spectral region, peaking around 400 nm, is also discerned. This band could be attributed to the π^*–π relaxation of free DBM-OH moiety (see Fig. 6c) and is too weak to be observed in the Eu-DBM-Si hybrid. These results suggest that DBM-Si is a more efficient sensitizer for the Eu^{3+} luminescence than DBM-OH and that the intramolecular energy transfer from DBM-Si ligand is more complete.

3.6. PL intensities and symmetry properties

For the sake of further investigation on the luminescence intensities of Eu-DBM and Eu-DBM-Si in detail, the $^5D_0 \rightarrow {}^7F_2$ emission

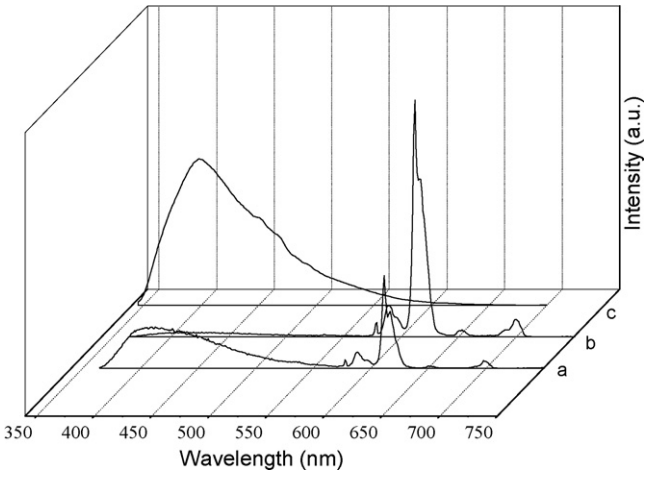

Fig. 6. PL spectra of Eu-DBM (0.5%) (a, λ_{ex} = 350 nm), Eu-DBM-Si (0.5%) (b, λ_{ex} = 350 nm) and DBM-Si (0.5%) (c, λ_{ex} = 330 nm).

Table 1
Photophysical data of Eu-DBM and Eu-DBM-Si in solid state.

	Eu-DBM	Eu-DBM-Si
I_{02}	531,848	1,941,439
R	6.40	8.22
Ω_2 (10^{-20} cm^2)	10.97	14.11
Ω_4 (10^{-20} cm^2)	1.47	2.17
τ (ms)	0.17	0.32
τ_{exp}^{-1}(s^{-1})	5,882	3,125
A_{rad} (s^{-1})	425	536
A_{nrad} (s^{-1})	5,457	2,589
q (%)	7.2	17.2
Φ (%)	3.8	8.2
$n_w/\pm 0.1$	5.6	2.5

I_{02}, emission intensities of $^5D_0 \rightarrow {}^7F_2$ transition; R, the intensity ratios of $^5D_0 \rightarrow {}^7F_2$ to $^5D_0 \rightarrow {}^7F_1$; Ω_λ, experimental intensity parameters; τ, decay times; A_{rad}, radiative decay rates; A_{nrad}, nonradiative decay rates; q, emission quantum efficiencies of the $^5D_0$ Eu^{3+} excited state calculated from the decay times and the emission intenties; Φ, absolute emission quantum yields measured at the room temperature.

intensity was compared for both the materials. Their relative emission intensities of $^5D_0 \rightarrow {}^7F_1$ transition (I_{01}) and $^5D_0 \rightarrow {}^7F_2$ transition (I_{02}) are listed in Table 1, which are obtained from the corresponding deconvolution results in the emission spectra. In comparison with Eu-DBM, the I_{02} value of Eu-DBM-Si increases ca. four times when the complex was covalently bonded into silicon dioxide host, implying that in Eu-DBM a quenching of the europium luminescence can be induced owing to the electron-phonon couplings with OH oscillator of ligands. However, upon functionalizing the ligand DBM-OH, the above shortcoming can be well overcome.

In addition, it is well known that the $^5D_0 \rightarrow {}^7F_2$ transition is a typical electric dipole transition and strongly varies with the local symmetry of Eu^{3+} ion, while the $^5D_0 \rightarrow {}^7F_1$ transition corresponds to a parity-allowed magnetic dipole transition, which is practically independent of the host material. Therefore, the intensity ratio (R) of $^5D_0 \rightarrow {}^7F_2$ to $^5D_0 \rightarrow {}^7F_1$ is sensitive to the symmetry around Eu^{3+} ion and gives valuable information about the chemical microenvironment change of anions coordinating the Eu^{3+} ion [52]. When the R value is higher, the Eu^{3+} ion occupies a site of lower symmetry without an inversion center (a more asymmetric local environment). However, this ratio is also influenced by other factors, such as the polarizability of the ligands [53,54]. The intensity ratios for both the materials are also listed in Table 1. By comparison, it can be observed that the R value for Eu-DBM-Si is higher than that of the hybrid material Eu-DBM, which indicates that the local symmetry changed upon grafting the complex into matrices and that a more asymmetric environment was occupied by the Eu^{3+} ion in Eu-DBM-Si than that in Eu-DBM, probably due to the effect of confinement.

3.7. Luminescence decay times

The luminescence decay profiles for Eu-DBM and Eu-DBM-Si (not shown) are fitted with single exponentials, from which the room temperature luminescence decay times can be estimated that all the Eu^{3+} ions locate in the same average environments in obtained hybrid materials. The resulting lifetimes are also listed in Table 1. It can be seen that the lifetime in Eu-DBM is much shorter than that in Eu-DBM-Si, which is probably ascribed to a quenching by OH groups from the ligands near the Eu^{3+} ion.

3.8. Quantum efficiencies (q)

In order to further discuss the photophysical properties of the resulting materials, the luminescence quantum efficiency q of the $^5D_0$ Eu^{3+} ion and the number of water molecules n_w coordinated to

the Eu^{3+} ion in Eu-DBM and Eu-DBM-Si were calculated based on the emission spectra and lifetimes of the $^5D_0$ emitting level [55], respectively, which are listed in Table 1. It can be seen that the lower number of water molecules in Eu-DBM-Si than that in Eu-DBM, indicates an alteration occurred in the Eu(III) first coordination shell after the ligand was functionalized and the corresponding complex was covalently grafted into silica. Moreover, the quantum yields of europium complex measurements support the qualitative observations made from the emission spectra and are also summarized in Table 1. Each quantum yield value is the average of three independent measurements. The absolute emission quantum yields (Φ) estimated for Eu-DBM-Si and Eu-DBM are 8.2 and 3.8%, respectively. As the same situation observed for the Φ values, the q value for the former hybrid material is much higher than that for the latter. Since the absolute emission quantum yield is defined as the ratio between the number of emitted and absorbed photons, the value of Φ is less than or equal to the value of q. The similar phenomena have been observed in other literature [19,56]. The low quantum yield and quantum efficiency of the hybrid material Eu-DBM may be caused by the higher non-radiative transition probability (A_{nrad}), which is arised from the luminescence quenching of the $^5D_0$ emitting level by OH oscillators of ligand or the water molecules in the first coordination sphere (the central Eu^{3+} ion plus the attached ligands of a coordination compound). However, upon functionalizing the ligand, OH oscillators can be efficiently avoided and the number of water molecules can be reduced due to its larger steric hindrance effect, which leads us to conclude that there is a more efficient intramolecular energy transfer process (from ligand-to-Eu(III)) in Eu-DBM-Si than in Eu-DBM, consistent with the results of emission spectra.

3.9. Judd-Ofelt parameters

As well known, Judd-Ofelt theory is a useful tool for analyzing f–f electronic transitions [57–59]. Interaction parameters of ligand fields are given by the Judd-Ofelt parameters Ω_λ (where $\lambda = 2$, 4, and 6). And Ω_λ is particularly more sensitive to the symmetry and sequence of ligand fields [60]. The experimental intensity parameters (Ω_λ, $\lambda = 2$ and 4) were determined from the emission spectra for Eu^{3+} ion in Fig. 6 based on the $^5D_0 \rightarrow {}^7F_{2,4}$ electronic transitions and the $^5D_0 \rightarrow {}^7F_1$ magnetic dipole allowed transition as the reference [57,61–66]. The Ω_6 parameter was not determined since the $^5D_0 \rightarrow {}^7F_6$ transition could not be experimentally observed. Therefore, its influence on the depopulation of the $^5D_0$ excited state is neglected, and the radiative contribution is estimated based only on the relative intensities of the $^5D_0 \rightarrow {}^7F_{0-4}$ transitions. The Ω_2 and Ω_4 intensity parameters for Eu-DBM and Eu-DBM-Si are also shown in Table 1. It is worth noting that the value of the Ω_2 intensity parameter for Eu-DBM-Si is the higher than that of Eu-DBM, which might be interpreted as a consequence of the hypersensitive behavior of the $^5D_0 \rightarrow {}^7F_2$ transition. Therefore, the dynamic coupling mechanism is quite operative, suggesting that the Eu^{3+} ion is in a highly polarizable chemical environment in Eu-DBM-Si, in agreement with the above discussion results.

4. Conclusions

Luminescent, colorless, transparent and homogenous gelation hybrid materials were prepared by covalently bonding or physical doping with binary lanthanide complex $Eu(DBM\text{-}OH)_3{\cdot}2H_2O$. Compared to the general physical doped material hybrid Eu-DBM, the hybrid material Eu-DBM-Si exhibits a stronger emission of Eu^{3+} ion, higher quantum efficiency and yield, longer luminescent decay time. These conclusions were quantitatively stressed by calculating the emission quantum efficiency q of Eu^{3+} ion, absolute quantum yield and the experimental intensity parameters Ω_2. However, the interactions between the organic complex and the silica matrix still need further fundamental investigations.

Acknowledgements

This work is financially supported by the National Natural Science Foundation of China (grant nos. 20490210, 206301040, 20602035 and 20771099) and the MOST of China (grant no. 2006CB601103). L.S.F. thanks Fundação para a Ciência e Tecnologia (Portuguese agency) for post-doctoral grant (SFRH/BPD/5657/2001).

References

[1] V.M. Mukkala, M. Helenius, I. Hem milä, J. Kankare, H. Takalo, Helv. Chim. Acta 76 (1993) 1361–1378.
[2] J.-C.G. Bünzli, C. Piguet, Chem. Rev. 102 (2002) 1897–1928.
[3] M. Iwamuro, Y. Hasegawa, Y. Wada, K. Murakoshi, T. Kitamura, N. Nakashima, T. Yamanaka, S. Yanagida, Chem. Lett. (1997) 1067–1068.
[4] M.P.O. Wolbers, F.C.J.M. van Veggel, B.H.M. Snellink-Ruel, J.W. Hofstraat, F.A.J. Geurts, D.N.J. Reinhoudt, Chem. Soc. Perkin Trans. 2 (1998) 2141–2150.
[5] J. Kido, Y. Okamoto, Chem. Rev. 102 (2002) 2357–2368.
[6] B.I. Ipe, K. Yoosaf, K.G. Thomas, J. Am. Chem. Soc. 128 (2006) 1907–1913.
[7] T. Gunnlaugsson, J.P. Leonard, Chem. Commun. (2003) 2424–2425.
[8] S. Quici, M. Cavazzini, G. Marzanni, G. Accorsi, N. Armaroli, B. Ventura, F. Barigelletti, Inorg. Chem. 44 (2005) 529–537.
[9] N. Sabbatini, A. Mecati, M. Guardigli, J.M. Lehn, Coord. Chem. Rev. 123 (1993) 201–228.
[10] T. Jin, S. Tsutsumi, Y. Deguchi, K. Machida, G. Adachi, J. Electrochem. Soc. 142 (1995) L195–L197.
[11] L.R. Matthews, E.T. Kobbe, Chem. Mater. 5 (1993) 1697–1700.
[12] F. Embert, A. Mehdi, C. Reye, R.J.P. Corriu, Chem. Mater. 13 (2001) 4542–4549.
[13] A.C. Franville, D. Zambon, R. Mahiou, Y. Troin, Chem. Mater. 12 (2000) 428–435.
[14] K. Binnemans, P. Lenaerts, K. Driesen, C. Görller-Walrand, J. Mater. Chem. 14 (2004) 191–195.
[15] P. Lenaerts, A. Storms, J. Mullens, J. D'Haen, C. Görller-Walrand, K. Binnemans, K. Driesen, Chem. Mater. 17 (2005) 5194–5201.
[16] K. Driesen, R. Van Deun, C. Görller-Walrand, K. Binnemans, Chem. Mater. 16 (2004) 1531–1535.
[17] V. de Zea Bermudez, R.A. Sá Ferreira, L.D. Carlos, C. Molina, K. Dahmouche, S.J.L. Ribeiro, J. Phys. Chem. B 105 (2001) 3378–3386.
[18] L.D. Carlos, R.A. Sá Ferreira, J.P. Rainho, V. de Zea Bermudez, Adv. Funct. Mater. 12 (2002) 819–823.
[19] P.P. Lima, R.A. Sá Ferreira, R.O. Freire, F.A. Almeida Paz, L.S. Fu, S. Alves Jr., L.D. Carlos, O.L. Malta, Chem. Phys. Chem. 7 (2006) 735–746.
[20] H.R. Li, J. Lin, H.J. Zhang, H.C. Li, L.S. Fu, Q.G. Meng, Chem. Commun. (2001) 1212–1213.
[21] F.Y. Liu, L.S. Fu, J. Wang, Q.G. Meng, H.R. Li, J.F. Guo, H.J. Zhang, New J. Chem. 27 (2003) 233–235.
[22] H.R. Li, J.B. Yu, F.Y. Liu, H.J. Zhang, L.S. Fu, Q.G. Meng, C.Y. Peng, J. Lin, New J. Chem. 28 (2004) 1137–1141.
[23] L.D. Carlos, A.L.L. Videira, Phys. Rev. B 49 (1994) 11721–11728.
[24] V.A. Smirnov, O.E. Philippova, G.A. Sukhadolski, A.R. Khokhlov, Macromolecules 31 (1998) 1162–1167.
[25] V. Bekiari, G. Pistolis, P. Lianos, Chem. Mater. 11 (1999) 3189–3195.
[26] L.H. Wang, W. Wang, W.G. Zhang, E.T. Kang, W. Huang, Chem. Mater. 12 (2000) 2212–2218.
[27] C.Y. Yang, V. Srdanov, M.R. Robinson, G.C. Bazan, A.J. Heeger, Adv. Mater. 14 (2002) 980–983.
[28] K. Binnemans, C. Görller-Walrand, Chem. Rev. 102 (2002) 2303–2345.
[29] R. Van Deun, D. Moors, B. De Fré, K. Binnemans, J. Mater. Chem. 13 (2003) 1520–1522.
[30] S. Arenz, A. Babai, K. Binnemans, K. Driesen, R. Giernoth, A.V. Mudring, P. Nockemann, Chem. Phys. Lett. 402 (2005) 75–79.
[31] K. Lunstroot, K. Driesen, P. Nockemann, C. Görller-Walrand, K. Binnemans, S. Bellayer, J.L. Bideau, A. Vioux, Chem. Mater. 18 (2006) 5711–5715.
[32] L.L. Hench, J.K. West, Chem. Rev. 90 (1990) 33–72.
[33] G.D. Qian, M.Q. Wang, J. Phys. Chem. Solids 58 (1997) 375–378.
[34] P. Judeinstein, C. Sanchez, J. Mater. Chem. 6 (1996) 511–525.
[35] C. Sanchez, F. Ribot, L. Rozes, B. Alonso, Mol. Cryst. Liq. Cryst. 354 (2000) 731–746.
[36] C. Sanchez, G.J. de, A.A. Soler-Illia, F. Ribot, T. Lalot, C.R. Mayer, V. Cabuil, Chem. Mater. 13 (2001) 3061–3083.
[37] C. Sanchez, B. Julian, P. Belleville, M. Popall, J. Mater. Chem. 15 (2005) 3559–3592.
[38] P. Escribano, B. Julian-Lopez, J. Planelles-Arago, E. Cordoncillo, B. Viana, C. Sanchez, J. Mater. Chem. 18 (2008) 23–40.
[39] H.H. Li, S. Inoue, K. Machida, G. Adachi, Chem. Mater. 11 (1999) 3171–3176.

[40] L.N. Sun, H.J. Zhang, L.S. Fu, F.Y. Liu, Q.G. Meng, C.Y. Peng, J.B. Yu, Adv. Funct. Mater. 15 (2005) 1041–1048.
[41] C.Y. Peng, H.J. Zhang, J.B. Yu, Q.G. Meng, L.S. Fu, H.R. Li, L.N. Sun, X.M. Guo, J. Phys. Chem. B 109 (2005) 15278–15287.
[42] L.N. Sun, H.J. Zhang, C.Y. Peng, J.B. Yu, Q.G. Meng, L.S. Fu, F.Y. Liu, X.M. Guo, J. Phys. Chem. B 110 (2006) 7249–7258.
[43] A.H. Chen, W.B. Kuo, C.W. Chen, J. Chin. Chem. Soc. 50 (2003) 123–127.
[44] N. Sabbatini, A. Mecati, M. Guardigli, V. Balzani, J.M. Lehn, R. Zeissel, R. Ungaro, J. Lumin. 48 & 49 (1991) 463–468.
[45] M. Kawa, J.M.J. Fréchet, Chem. Mater. 10 (1998) 286–296.
[46] T. Förster, Z. Naturforsch. A 4 (1949) 321–327.
[47] W.F. Sager, N. Filipescu, F.A. Serafin, J. Phys. Chem. 69 (1965) 1092–1100.
[48] I.B. Berlman, Energy Transfer Parameters of Aromatic Compounds, Academic Press, New York, 1973.
[49] S. Sato, M. Wada, Bull. Chem. Soc. Jpn. 43 (1970) 1955–1962.
[50] G.A. Crosby, R.E. Whan, R.M. Alire, J. Chem. Phys. 34 (1961) 743–748.
[51] N. Filipescu, W.F. Sager, F.A. Serafin, J. Phys. Chem. 68 (1964) 3324–3346.
[52] A.F. Kirby, D. Foster, F.S. Richardson, Chem. Phys. Lett. 95 (1983) 507–512.
[53] O.L. Malta, L.D. Carlos, Quim. Nova 26 (2003) 889–895.
[54] T.R. Zhang, C. Spitz, M. Antonietti, C.F.J. Faul, Chem. Eur. J. 11 (2005) 1001–1009.
[55] R.M. Supkowski, W.D. Horrocks Jr., Inorg. Chim. Acta 340 (2002) 44–48.
[56] M. Fernandes, V. de Zea Bermudez, R.A. Sá Ferreira, L.D. Carlos, A. Charas, J. Morgado, M.M. Silva, M.J. Smith, Chem. Mater. 19 (2007) 3892–3901.
[57] B.R. Judd, Phys. Rev. 127 (1962) 750–761.
[58] G.S. Ofelt, J. Chem. Phys. 37 (1962) 511–519.
[59] M.H.V. Werts, R.T.F. Jukes, J.W. Verhoeven, Phys. Chem. Chem. Phys. 4 (2002) 1542–1548.
[60] S. Biju, D.B. Ambili Raj, M.L.P. Reddy, B.M. Kariuki, Inorg. Chem. 45 (2006) 10651–10660.
[61] O.L. Malta, M.A. Couto dos Santos, L.C. Thompson, N.K. Ito, J. Lumin. 69 (1996) 77–84.
[62] O.L. Malta, H.F. Brito, J.F.S. Menezes, F.R. Gonçalves e Silva, S. Alves Jr., F.S. Farias Jr., A.V.M. Andrade, J. Lumin. 75 (1997) 255–268.
[63] G.F. de Sá, O.L. Malta, C. de Mello Donegá, A.M. Simas, R.L. Longo, P.A. Santa-Cruz, E.F. da Silva Jr., Coord. Chem. Rev. 196 (2000) 165–195.
[64] E.E.S. Teotonio, J.G.P. Espínola, H.F. Brito, O.L. Malta, S.F. Oliveria, D.L.A. de Foria, C.M.S. Izumi, Polyhedron 21 (2002) 1837–1844.
[65] C.A. Kodaira, A. Claudia, H.F. Brito, M.C.F.C. Felinto, J. Solid State Chem. 171 (2003) 401–407.
[66] J.C. Boyer, F. Vetrone, J.A. Capobianco, A. Speghini, M. Bettinelli, J. Phys. Chem. B 108 (2004) 20137–20143.